05

Certain peculiarities of EPR spectra of Tb^{3+} in yttrium-aluminum garnet at a frequency of 94 GHz

© G.R. Asatryan[1,2], R.A. Babunts[1], N.G. Romanov[1], D.D. Kramuschenko[1], K.L. Ovanesyan[2], A.G. Petrosyan[2]

[1] Ioffe Institute,
St. Petersburg, Russia
[2] Institute for Physical Research, Armenian Academy of Sciences,
0203 Ashtarak, Republic of Armenia
E-mail: hike.asatryan@mail.ioffe.ru

Received December 26, 2024
Revised December 28, 2024
Accepted December 31, 2024

Terbium-containing crystals of yttrium-aluminum garnet, apart from EPR Tb^{3+} ions, located in the yttrium position in regular environment, demonstrated EPR of terbium centers, the initial splitting of the non-Kramer's quasidoublet levels of which is close to 94 GHz photon energy. They are ions of terbium with antisite defects Y_{Al} near them (yttrium ions in octahedral positions of aluminum). Using magnetic field modulation, operating frequency modulation and electron spin echo, the peculiarities of the EPR spectra were studied for such centers in low magnetic fields. The EPR spectra are also found for new centers with the hyperfine structure specific for Tb^{3+} and low intensity (approximately 0.05 % compared to the main centers). The number of the lines and the symmetry of these centers indicate their association with Tb^{3+} ions, substituting for Al^{3+} ions in the octahedral sites of the YAG crystal lattice.

Keywords: Electron paramagnetic resonance, yttrium-aluminum garnet, rare earth elements, antisite defects

DOI: 10.61011/PSS.2025.03.60877.354

1. Introduction

Crystals of yttrium-aluminum garnet $Y_3Al_5O_{12}$ (YAG), containing terbium ions, find multiple applications in quantum electronics and optoelectronics, are used as scintillators in nuclear physics and medical diagnostics, are promising systems for quantum computing [1–5].

Most rare earth elements, including terbium, are embedded in the YAG lattice in the dodecahedral c-position. EPR of non-Kramer's Tb^{3+} ions in YAG was studied in Refs. [6–8]. It was shown that apart from the main centers, where Tb^{3+} substitutes for Y^{3+} and is in the regular environment, there are some terbium centers, the environment of which contains antisite defects, causing disturbances of the crystalline field — Y_{Al} (yttrium ions in the octahedral positions of aluminum) or Al_Y (aluminum ions in dodecahedral positions of yttrium). The splitting of the non-Kramer's quasidoublet Δ of these centers is larger or smaller, respectively, than the value $\Delta = 81.1$ GHz of the main centers of terbium [8]. For one of these centers designated as Tb^{3+}(I) in [6,7] or as Tb^{3+}(B3) in [8], the initial splitting Δ is approximately equal to the energy of the 94 GHz microwave quantum and EPR is observed in the zero field and low magnetic fields.

Similar to Y^{3+} ions forming antisite defects Y_{Al}, some impurity rare-earth ions in YAG may possibly be located in the octahedral a-sites, substituting at Al^{3+} ions. Optical spectra of Er^{3+} ions in aluminum positions in YAG were observed in [9]. Ref. [10] reported observation of EPR spectra of Ce^{3+} ions in Al^{3+} positions in crystals of $Lu_3Al_5O_{12}$ (LuAG), and in Ref. [11] EPR of another rare-earth ion, Ho^{3+}, in octahedral positions of aluminum in YAG crystals was reported.

This paper is devoted to a more detailed study of paramagnetic centers of terbium in YAG:Tb crystals by using high-frequency EPR at 94 GHz in continuous (using both magnetic field modulation and operating frequency modulation) and pulse (electron spin echo, ESE) modes.

2. Specimens and experiment procedure

Single crystals of $Y_3Al_5O_{12}$:Ce,Tb were grown in molybdenum containers in neutral-recovery atmosphere (Ar/H_2) using highly pure (99.99 %) oxides at a temperature of about 1940 °C by vertical directed crystallization [12,13] in the Institute for Physical Research, National Academy of Sciences, Republic of Armenia (Ashtarak, Republic of Armenia). The crystals were grown along the crystallographic axis $\langle 100 \rangle$. The cerium content in the crystals was 0.12 at.% relative to yttrium, and the terbium concentration was estimated to be approximately 0.1 at.%. The samples for EPR measurements were cut from central, most homogeneous areas of grown crystals.

EPR spectra at 94 GHz were recorded in continuous wave (CW) mode, and via electron spin echo, in the temperature range 1.5–40 K using high frequency EPR-ODMR spectrometer developed in the Ioffe Institute [14,15]. During operation in continuous mode, except for modulation of magnetic field, operating frequency modulation was

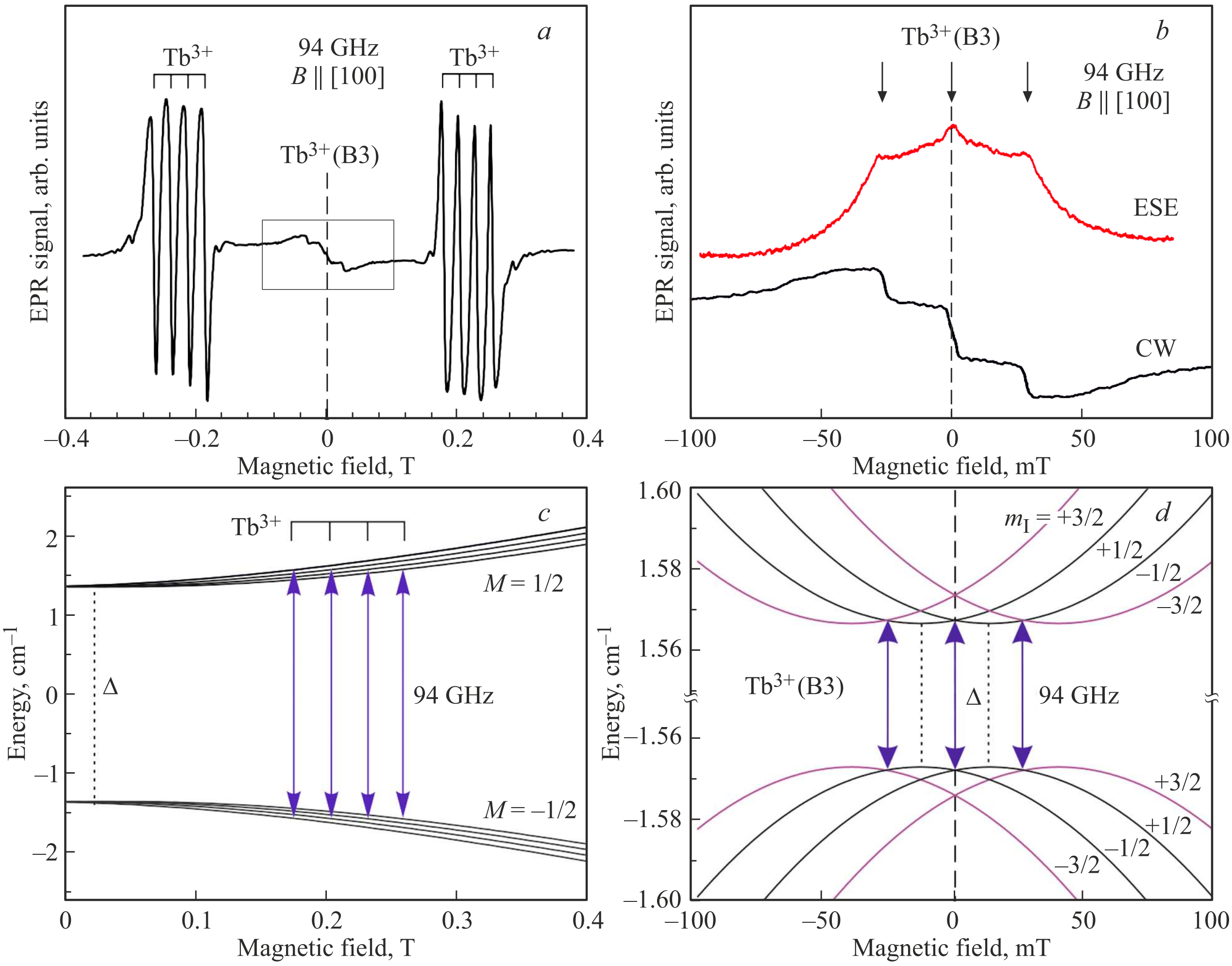

Figure 1. (*a*) EPR spectrum recorded in CW mode at frequency of 94 GHz with field modulation. (*b*) EPR spectra near zero field recorded at orientation of crystal $[100] \parallel \mathbf{B}$ in CW mode with modulation of magnetic field and in pulse mode using electron spin echo (ESE). (*c, d*) Schemes of energy levels of Tb^{3+} and Tb^{3+}(B3) centers, respectively, at $\mathbf{B} \parallel [100]$; M and m_I are quantum numbers of projection of electron and nuclear magnetic moments.

used [16]. This method is especially effective for paramagnetic centers, the energy of levels of which weakly depends on the magnetic field. Automatic switching of sensitivity of the spectrometer lock-in detector using a specially designed control software provided wide dynamic range in recording of the spectra, which exceeded 120 dB [17].

3. Experimental results and discussion

The EPR spectrum of YAG:Tb crystals, recorded at a frequency of 94 GHz at a temperature of 1.7 K and orientation $\mathbf{B} \parallel [100]$, is shown in Figure 1, *a*. This spectrum was recorded with the change of magnetic field direction and smooth zero crossing. The spectrum includes signals of the main Tb^{3+} centers, and also the lines near zero magnetic field (in fields from -0.1 to 0.1 T), which belong to centers Tb^{3+}(B3). As shown in Figure 1, *b*, EPR spectra of such centers may be recorded both in CW mode with magnetic field modulation and by ESE.

Electronic configuration of Tb^{3+} is $4f^8$, the ground state of a free ion is $^7F_6$. Tb^{3+} is a non-Kramers ion, and its EPR spectra may be described by a spin Hamiltonian with the effective spin $S = 1/2$, anisotropic g-factor ($g_\perp \sim 0$) and the splitting of levels in zero magnetic field Δ [6,18]. Terbium has one stable isotope ^{159}Tb with a natural content of 100 % and nuclear spin $I = 3/2$, therefore, in its EPR spectra each electronic transition is split into four hyperfine structure (HFS) lines. This makes it possible to reliably identify terbium centers.

Energy levels of the ground state of Tb^{3+}-centers in YAG can be calculated using formula

$$E = \pm 1/2\left[(g_\parallel \mu_B B \cos\theta + A m_I)^2 + \Delta^2\right]^{1/2}, \qquad (1)$$

where μ_B is the Bohr magneton, Δ is the level splitting in zero field, A is the constant of hyperfine interaction, $m_I = -3/2,\ -1/2,\ 1/2,\ 3/2$ is the magnetic quantum number of nucleus, θ is the angle between the axis of

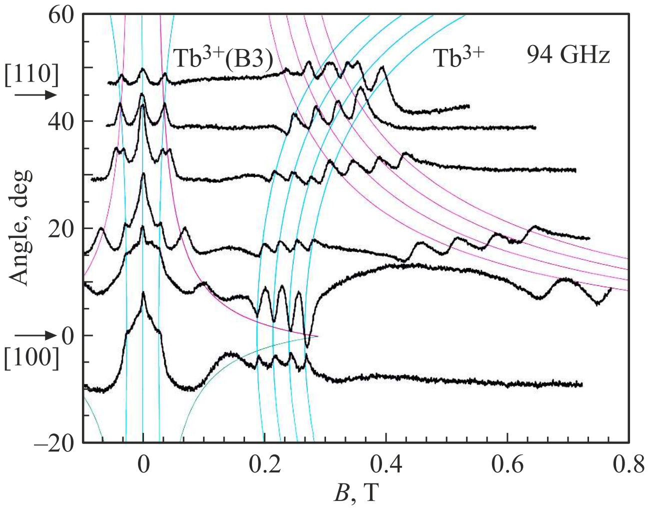

Figure 2. Orientation dependence of ESE spectra in YAG:Tb crystals in the plane (100). $\nu = 94\,\mathrm{GHz}$, $T = 1.52\,\mathrm{K}$. $\theta = 0$ corresponds to orientation $\mathbf{B} \parallel [100]$.

the center and the magnetic field **B**. $g_\perp = 0$. The axes of Tb^{3+}-centers in YAG are oriented along one of three directions of $\langle 100 \rangle$ type. Energy levels and EPR-transitions at a frequency of 94 GHz for the main Tb^{3+} centers and centers Tb^{3+}(B3) with $\Delta \sim 94\,\mathrm{GHz}$ are shown in Figure 1, *c* and *d*. The following parameters were used in the calculation $g = 15.65$, $\Delta = 81.1\,\mathrm{GHz}$, $A = 5.5\,\mathrm{GHz}$ were used for Tb^{3+} and $g = 15.60$, $\Delta = 94\,\mathrm{GHz}$, $A = 5.5\,\mathrm{GHz}$ for Tb^{3+}(B3) [8].

The orientation dependences of the resonance magnetic fields of „defective" centers Tb^{3+}(B3) are similar to the corresponding dependences for the main center Tb^{3+}, as it follows from Figure 2, which shows the calculated angular dependences for these centers in the (100) plane and the EPR spectra recorded by ESE during crystal rotation around the axis close to [001].

The signals in the zero field region are clearly visible in the EPR spectra recorded using low-frequency (680 Hz) modulation of the operating frequency (see Figure 3, *a*). These spectra were obtained at a temperature of 1.7 K with an arbitrary crystal orientation. The part of the spectrum identified in Figure 3, *a* is shown in enlarged scale in Figure 3, *b*.

The spectrum in Figure 3, *a* contains two intense hyperfine quartets of the main Tb^{3+}-centers, the position of which makes it possible to determine the orientation of axes in the corresponding centers using angular dependences calculated with the known parameters [8]. Angles θ_1 and θ_2 defined in this manner are equal to 36 and 57 °. Since the axes of Tb^{3+}-centers in YAG are oriented along one of the three crystalline axes of the $\langle 100 \rangle$ type and are mutually orthogonal, the angle $\theta_3 = 78^\circ$ for the third center was defined using the relation $\cos^2(\theta_1) + \cos^2(\theta_2) + \cos^2(\theta_3) = 1$. The same angles can be used to calculate the angular dependences of the Tb^{3+}(B3) centers.

The calculated dependences of resonance fields of Tb^{3+}(B3) centers and EPR transitions at 94 GHz for all three angles are shown in Figure 3, *b*. The horizontal line corresponds to the frequency of 94 GHz. The number and position of the experimentally observed EPR lines of centers Tb^{3+}(B3) marked in Figure 3, *b* with dots agree well with the calculation results. This proves the correctness of the determined parameters and confirms the conclusion that the symmetry of the Tb^{3+}(B3) and Tb^{3+} centers is the same.

It should be noted that intense EPR signals of Tb^{3+}-centers in low magnetic fields are observed near the point of crossing of hyperfine sublevels $m_I = \pm 1/2$ and $m_I = \pm 3/2$, calculated using (1) and shown in Figure 1, *d* and Figure 3, *b*. From the calculation it follows that if the constant of hyperfine interaction *A* does not change noticeably, this point does not change its position for the terbium centers with various initial splittings Δ. When the operating frequency of the spectrometer changes from 93.75 GHz to 94.25 GHz, the EPR lines of the main Tb^{3+} centers are shifted to higher fields, and their position corresponds to the calculated one. At the same time, the EPR signals of Tb^{3+}(B3) centers continue to be registered in the same fields. Apparently, there is a distribution of the values of the initial splittings Δ for Tb^{3+}(B3) centers, making it possible to observe EPR-transitions in the point of crossing of the hyperfine sublevels at these various frequencies. It is of interest to study EPR spectra of other terbium centers described in [8] by changing the operating frequency of the EPR spectrometer near the zero-field splitting value.

In papers [6–8] Tb^{3+} and Ce^{3+} centers with antisite defects of the Y_{Al} or Al_Y type in the environment of the paramagnetic center were considered. The distances were calculated from the dodecahedral site, occupied by the impurity ion, to the nearest positions of Al or Y, which have a common oxygen ion with the paramagnetic center, and directly impact the distortion of the crystalline field in the area of its location. It was shown that for ten Al sites close to Tb^{3+} there are three values of distances [7], and for four close sites of Y^{3+} there are two values [8]. The presence of paramagnetic centers with altered values of the splitting of the non-Kramer's quasidoublet is possible for two reasons. Firstly, due to the considerable difference of the ion radii of the interchangeable ions of aluminum and yttrium ($R^{3+}_{\mathrm{Al}(6)} = 0.53\,\text{Å}$, $R^{3+}_{\mathrm{Y}(8)} = 1.02\,\text{Å}$), the crystal lattice in the environment of the antisite defect is strongly distorted, and it is naturally to assume that deformation of the crystalline lattice near the paramagnetic center is not limited to the nearest defect sites accounted for previously. The crystal field will be distorted due to the presence of antisite defects located at farther distances. It is also possible that there are paired antisite defects next to Tb^{3+} — both Al^{3+} in place of Y^{3+} and Y^{3+} in place of Al^{3+}. Secondly, the number of centers with the antisite defect Y_{Al} in the immediate environment of Tb^{3+} (10) determined in [7] does not coincide with the

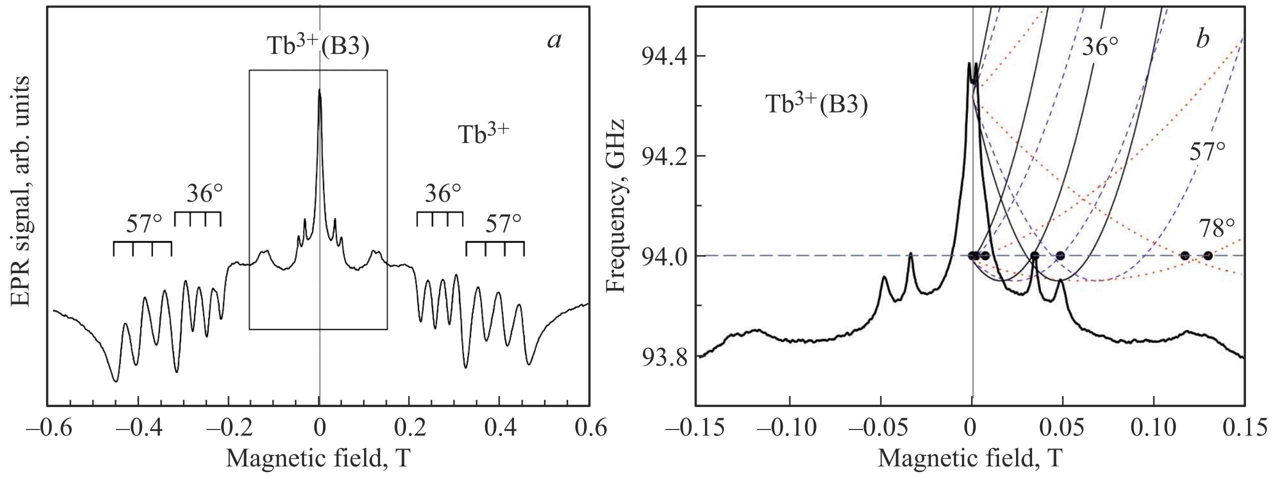

Figure 3. (*a*) EPR spectra recorded in YAG:Tb crystal with low frequency (680 Hz) modulation of operating frequency 94 GHz. Field range is highlighted, where signals of Tb^{3+}(B3) centers are observed. (*b*) EPR spectrum of Tb^{3+}(B3) centers in the field range highlighted on the panel (*a*), and calculated dependences of resonance frequencies on the magnetic field for three magnetically nonequivalent centers at $\theta = 36°$, $57°$ and $78°$.

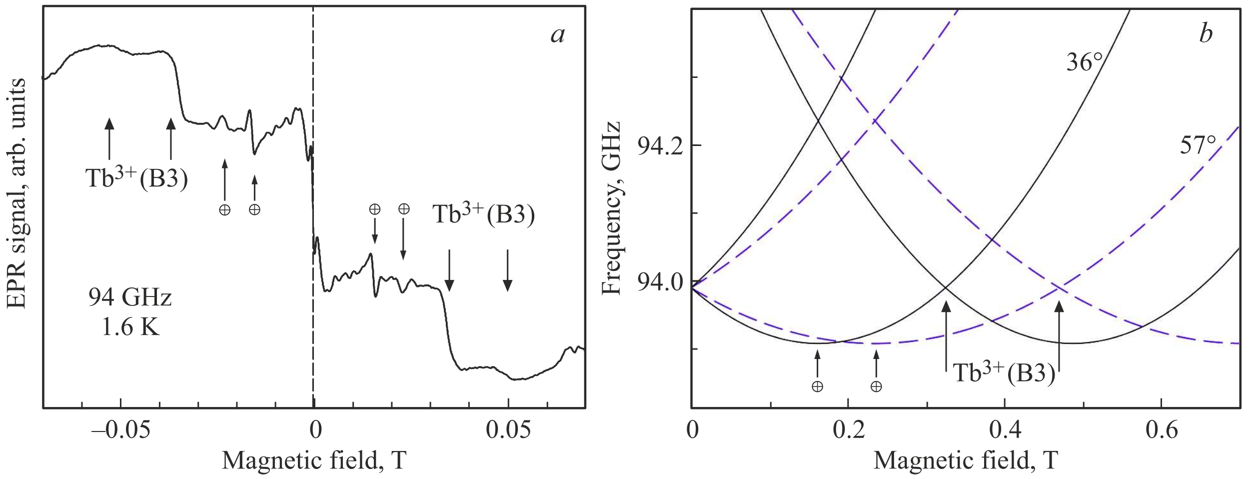

Figure 4. (*a*) 94 GHz EPR spectra of YAG:Tb crystal, recorded with magnetic field modulation. The crystal orientation is the same as in Figure 3. (*b*) Field dependence of level splitting for terbium centers Tb^{3+}(B3), calculated for two angles between the axis of the center and the magnetic field — 36° (solid lines) and 57° (dashed lines). The points indicate the position of new resonance signals.

number of magnetically nonequivalent centers (3), observed in the experiment. For orientations other than [100], in principle, all ten centers may be resolved. And when the antisite defect Al_Y is located near the paramagnetic ion Tb^{3+}, all four centers may be resolved. To finally establish the reason for diversity of the terbium centers, detailed EPR studies are necessary at different frequencies, including measurements of orientation dependences for all centers.

Figure 4, *a* shows EPR spectrum recorded with modulation of magnetic field in YAG:Tb at the same orientation of the crystal as the spectra shown in Figure 3, *a* and Figure 4, *b* — the dependence of the resonance frequency on the magnetic field for centers Tb^{3+}(B3), calculated at $\theta = 36$ and $57°$. In addition to the EPR lines, which are marked in Figure 4 with bold arrows and match the lines shown in Figure 3, *b*, narrower (1.2 mT) lines are observed in zero field and in magnetic fields, which correspond to extrema of frequency-field dependence, i.e. in the fields, where the energy of levels does not depend on the field. Similar lines were observed previously in EPR spectra of impurity ions Tm^{3+} in synthetic forsterite [19] and were explained by strong saturation of resonance transition due to drastic increase of effective time of phase relaxation in the magnetic field, where the linear Zeeman effect is absent. In contrast to the spectrum given in Figure 4, *a*, in paper [19] the sign of narrow EPR lines in zero field was opposite to the sign of lines in the magnetic field. To understand the nature of such signals in YAG:Tb crystals, the additional research is necessary.

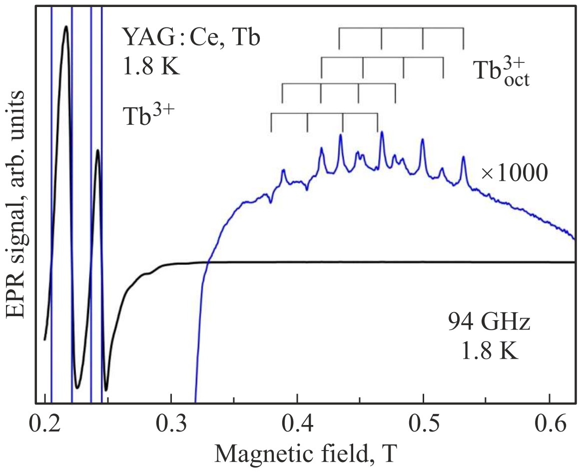

Figure 5. EPR spectrum at a frequency of 94 GHz in YAG:Ce,Tb crystal at a temperature of 1.8 K. In the part of the spectrum shown in a 1000-fold magnification, EPR lines of four magnetically nonequivalent centers are marked and designated as Tb$^{3+}_{\text{oct}}$.

4. Octahedral centers Tb^{3+} in YAG

When studying EPR of YAG:Tb crystals at a frequency of 94 GHz, new EPR signals were found with the HFS specific for terbium, the amplitude of which was much smaller than for the main Tb^{3+} centers (about 0.02 %). This was possible due to program switching of the spectrometer sensitivity, which provided a huge dynamic range (c.a. 120 dB) [17] when registering spectra and a signal-to-noise ratio ~ 10000. By increasing the scale of the already recorded spectrum vertically by 1000 times, it was possible to see the EPR spectra of new centers, also related to terbium ions. Such a spectrum for an arbitrary orientation of the crystal in the magnetic field is shown in Figure 5.

In the garnet structure 16 Al^{3+} ions are located in an octahedral environment of oxygen ions (a-positions with local symmetry C_{3i}). Oxygen octahedrons coordinating a-sites are distorted along the common axis [111] and are turned around it by equal angles ($\alpha \sim 28^\circ$), forming eight nonequivalent positions. On each spatial diagonal of the unit cell of $Y_3Al_5O_{12}$ crystals there are two Al^{3+} ions in octahedral coordination. For arbitrary orientation of the external magnetic field for centers with axial symmetry along $\langle 111 \rangle$, there are four magnetically nonequivalent positions, which become equivalent at field orientation along [001]. At $\mathbf{B} \parallel [110]$ three EPR signals must be observed, and at $\mathbf{B} \parallel [111]$ — one. The number of experimentally recorded magnetically nonequivalent positions for centers denoted as Tb$^{3+}_{\text{oct}}$ is equal to four. This corresponds to the assumption on localization of the paramagnetic center in the octahedral a-sites of the YAG lattice and orientation of the magnetic axes of centers along the crystal axes $\langle 111 \rangle$.

A part of the orientation dependence of EPR spectra of Tb$^{3+}_{\text{oct}}$ centers in the (011) plane is given in Figure 6, *a*. Due to overlapping of these signals with much more intense EPR spectra of terbium centers in dodecahedral positions, the angular dependence may be recorded only in the narrow range of angles. The points correspond to the centers of gravity of the HFS quartets, the lines are result of calculation for Tb^{3+} centers with axes of the $\langle 111 \rangle$ type and parameters $g = 15.8$, $\Delta = 73.45$ GHz, $A = 4.2$ GHz.

The orientation dependence shown in Figure 6, *a* highly differs from that of the main Tb^{3+} centers with the $\langle 100 \rangle$ type axes [6]. At $[100] \parallel \mathbf{B}$ the lines of all centers converge as it should be for the centers localized in octahedral sites. When rotating in the (011) plane, the lines of two of four such Tb^{3+} centers must coincide, as it is observed in the experiment. Figure 6, *b* shows the EPR spectrum in the orientation close to [100].

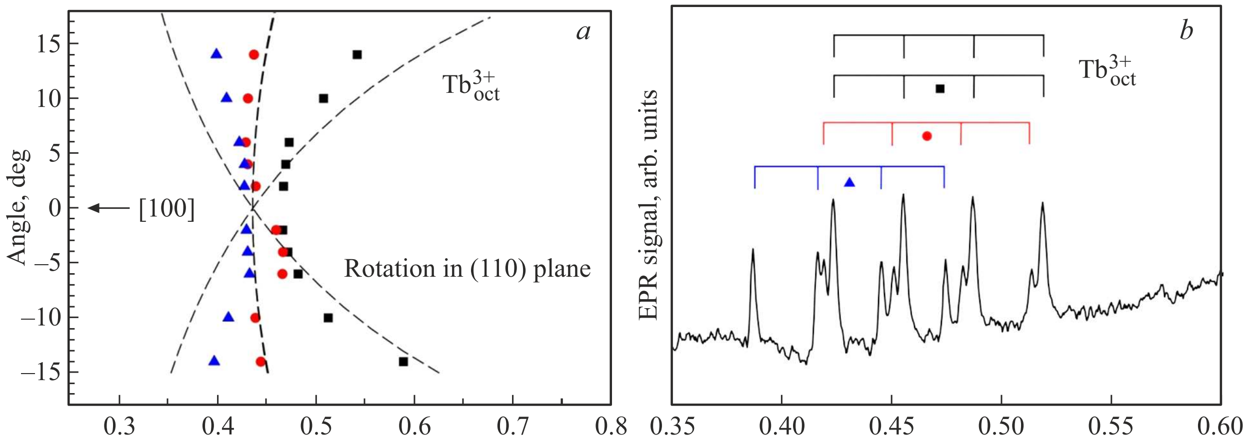

Figure 6. (*a*) Orientation dependence of EPR spectra of Tb$^{3+}_{\text{oct}}$ centers in (100) plane. The points indicate the positions of centers of gravity of the HFS quartets in the EPR spectra. The curves are the result of calculation for Tb^{3+} in the octahedral positions of Al. (*b*) EPR spectrum in orientation close to $[100] \parallel \mathbf{B}$. The calculated positions of EPR lines are marked.

Thus, the analysis of new EPR spectra of yttrium-aluminum garnet crystals with terbium makes it possible to assume that some Tb^{3+} ions occupy octahedral sites of YAG lattice, substituting at the same time ions Al^{3+}, as well as in the case of substitution of some octahedral a-sites with Al ions Y^{3+}. Low intensity of EPR signals of such octahedral terbium centers is caused by low probability of their formation.

5. Conclusion

The study of EPR spectra of yttrium-aluminum garnet crystals with terbium impurity, recorded in zero and low magnetic fields using electron spin echo, modulation of magnetic field and also modulation of microwave frequency made it possible to study the features of terbium centers with initial splitting near 94 GHz. Using automatic switching of sensitivity of the lock-in detector expanding the dynamic range when recording EPR spectra, new spectra of terbium centers were found with axes of type $\langle 111\rangle$, the analysis of which makes it possible to assume that a small part of impurity terbium ions in the garnet occupies the octahedral a-sites of YAG lattice, replacing Al^{3+} ions.

Funding

The work was carried out with financial support of the Russian Science Foundation under project No. 23-12-00152, https://rscf.ru/project/23-12-00152/ (R.A. Babunts, D.D. Kramuschenko) and State Science Committee, Republic of Armenia, under project No. 1-6/23-I/IPR (K.L. Ovanesyan, A.G. Petrosyan).

Conflict of interest

The authors declare that they have no conflict of interest.

References

[1] A. Kaminskii. Laser Crystals. Their Physics and Properties. Springer, Berlin (1990).
[2] V. Bachmann, C. Ronda, A. Meijerink. Chem. Mater. **21**, 2077 (2009).
[3] Y.S. Lin, R.S. Liu, B.-M. Cheng. J. Electrochem. Soc. **152**, J41 (2005).
[4] A.C. Dujardin, E. Auffray, E. Bourret-Courchesne, P. Dorenbos, P. Lecoq, M. Nikl, A.N. Vasil'ev, A. Yoshikawa, R. Zhu. IEEE Trans. Nucl. Sci. **65**, 1977 (2018).
[5] P. Slyushev, K. Xia, R. Reuter, M. Jamali, N. Zhao, N. Yang, C. Duan, N. Kukharchyk, A.D. Wieck, R. Kolesov, J. Wrachtrup. Nat. Commun. **5**, 3895 (2014).
[6] E.V. Edinach, Y.A. Uspenskaya, A.S. Gurin, R.A. Babunts, H.R. Asatryan, N.G. Romanov, A.G. Badalyan, P.G. Baranov. Phys. Rev. B **100**, 104435 (2019).
[7] G.R. Asatryan, E.V. Edinach, Y.A. Uspenskaya, R.A. Babunts, A.G. Badalyan, N.G. Romanov, A.G. Petrosyan, P.G. Baranov. Phys. Solid State **62**, *11*, 2110 (2020).
[8] G.R. Asatryan, G.S. Shakurov, N.G. Romanov, A.G. Petrosyan. Phys. Solid State **66**, *2*, 276 (2024).
[9] M.K. Ashurov, Y.K. Voronko, V. Osiko, A. Sobol, M. Timosheckin. Phys. Status Solidi A **42**, 101 (1977).
[10] V.V. Laguta, A.M. Slipenyuk, M.D. Glinchuk, I.P. Bykov, Yu. Zorenko, M. Nikl, J. Rosa, K. Nejezchleb. Radiat. Meas. **42**, 835 (2007).
[11] G.R. Asatryan, G.S. Shakurov, N.M. Lyadov, K.L. Hovhannesyan, A.G. Petrosyan. Opt. Memory Neural **32**, *Suppl. 3*, 356–351 (2023).
[12] A.G. Petrosyan. J. Cryst. Growth **139**, 372 (1994).
[13] A.G. Petrosyan, G.O. Shirinyan, K.L. Ovanesyan, A.A. Avetisyan. Krist. Techn. **13**, 43 (1978).
[14] E.V. Edinach, Yu.A. Uspenskaya, A.S. Gurin, R.A. Babunts, G.R. Asatryan, N.G. Romanov, A.G. Badalyan, P.G. Baranov. Phys. Solid State **61**, *10*, 1820 (2019).
[15] R.A. Babunts, A.G. Badalyan, A.S. Gurin, N.G. Romanov, P.G. Baranov, A.V. Nalivkin, L.Yu. Bogdanov, D.O. Korneev. Appl. Magn. Reson. **51**, 1125 (2020).
[16] R.A. Babunts, A.S. Gurin, Yu.A. Uspenskaya, H.R. Asatryan, D.O. Tolmachev, N.G. Romanov, A.G. Badalyan, P.G. Baranov. Tech. Phys. Lett. **46**, *5*, 454 (2020).
[17] R.A. Babunts, Y.A. Uspenskaya. Programma dlya uvelicheniya dinamicheskogo diapazona vysokochastotnogo EPR/ODMR spektrometra. Parent RF № 2022669432, zaregistrirovan 19.10.2022 (in Russia).
[18] J.M. Baker, B. Bleaney. Proc. Phys. Soc. A **68**, 257 (1955).
[19] N.K. Solovarov, V.F. Tarasov, E.V. Zharikov. JETP Lett. **104**, *2*, 94 (2016).

Translated by M.Verenikina